Preprint DOI: Posted on December 6, 2024
https://doi.org/10.1099/acmi.0.000906.v2

Quantification of *Pseudomonas aeruginosa* biofilms using electrochemical methods

Lily Riordan[1], Perrine Lasserre[2], Damion Corrigan[2], Katherine Duncan[1,3*]

[1] University of Strathclyde, Strathclyde Institute of Pharmacy and Biomedical Sciences, Glasgow, G4 0RE.

[2] University of Strathclyde, Department of Chemistry, Glasgow, G1 1BX.

[3] Newcastle University, Biosciences Institute, Faculty of Medical Sciences, Newcastle upon Tyne, NE2 4HH.

* Corresponding author email address: katherine.duncan@ncl.ac.uk

Abstract

Currently 2.29% of deaths worldwide are caused by antimicrobial resistance (AMR), compared to 1.16% from malaria, and 1.55% from human immunodeficiency virus and acquired immunodeficiency syndrome (HIV/AIDs). Furthermore, deaths resulting from AMR are projected to increase to more than 10 million *per annum* by 2050. Biofilms are common in hospital settings, such as medical implants and pose a particular problem as they have shown resistance to antibiotics up to 1000-fold higher than planktonic cells because of dormant states and reduced growth rates. This is compounded by the fact that many antibiotics target mechanisms of active metabolism and are therefore less effective. The work presented here aimed to develop a method for biofilm quantification which could be translated into the clinical setting, as well as used in the screening of antibiofilm agents. This was carried out alongside crystal violet staining, as a published point of reference. This work builds upon work previously presented by Dunphy, *et al.*, in which the authors attempted to quantify biofilm formation of *Pseudomonas aeruginosa* strain using hyperspectral imaging. Here, using electrochemical impedance spectroscopy and square wave voltammetry, the biofilm formation of two *P. aeruginosa* strains was detected within an hour after seeding *P. aeruginosa* on the sensor. A 40% decrease in impedance modulus was shown when *P. aeruginosa* biofilm had formed, compared to the media only control. As such, this work offers a starting point for the development of real-time biofilm sensing technologies, which can be translated into implantable materials.

Introduction

Biofilms are a community of bacteria, usually mixed species (1), with increased resistance to antibiotics, antimicrobials, and other biocides, often with minimum biocidal concentrations of 1000-fold higher than planktonic cells (2–5). Biofilms have been shown to afford the bacteria environmental protection (1), such as against shear stress and decreased nutrient availability (6). Mechanisms also include the creation of a physical barrier of extracellular polymeric substances (6–8) through sequestration of environmental and own molecules. This includes molecules and material from the environment in which the biofilm has formed, for examples within an animal host, materials such as red blood cells, platelets, and fibrin (8,9), as well as the cell's own "junk" DNA (1) and polysaccharides (10). Being in a biofilm allows bacteria to maintain a larger population number, as not all the bacteria are "exposed" to the outside of the biofilm, and therefore an antibiotic, at once, meaning that bacteria within a biofilm can withstand up to 1000 times higher antibiotic concentration than those not in biofilm (11,12), and additionally tolerate higher concentrations of organic compounds and salts (12). In a biofilm context, medical devices, and implants, such as catheters (13–15), grafts (13,16,17), and endoscopes (2,18), are a particular issue, as they provide a surface on which the biofilm can form (2,13). Biofilms create an obstacle for basic quantification, due to some cells entering dormancy (19), as well as cell biomass and other debris (6). There can also be challenges with interpreting quantification results, due to the biofilm architecture and micro-colony structure (1,20). Due to this, there are no standardised methods for biofilm quantification (1). There are three categories for biofilm quantification; biomass assays, which quantify the extracellular matrix (ECM), along with both living and dead cells; viability assays, which quantify the living cells only; and matrix quantification, which quantifies the components of the ECM only (21). Assays which capture the activity of pre-formed biofilms are of clinical relevance, as these replicate the clinical context as treatment occurs once a biofilm has become established (1).

Crystal violet (CV) staining was first used for the staining and quantification of biofilms by Fletcher in 1977 (22), and since then it has become the 'gold-standard' for biofilm quantification (1,4,9,21,23–31). CV staining can capture the activity of pre-formed biofilms and is one of the most common published quantification methods (6,31). CV stains all negatively charged surface molecules and polysaccharides (21), including anionic proteins,

nucleic acids, and lipopolysaccharides (1), and has the advantage of giving data on the total biofilm biomass, but also does not discriminate between live and dead cells (1,21). It has been demonstrated to be repeatable both within and between species (21) and can be quantified using a spectrophotometer by dissolving the crystal violet in a solvent (21,32,33). Prior to this advance, quantification was achieved using laborious and inaccurate microscopy cell counts both with and without CV staining (22,34). Despite its popular use, CV can give considerable background stain (23), though this can be overcome with washing steps (1,34). Background staining is also less significant with greater biofilm biomass, as is often observed when quantifying *Pseudomonas aeruginosa* (1,23). However, published methods all show variations in washing and quantification techniques (1,2,6,21,32,34–36). These variations include using no washing steps (34) or increased washing steps (23,29), as well as different solvents used to solubilise the CV, such as ethanol (4), glacial acetic acid (30), and isopropanol (29). Lastly, a recent review found that 75% of studies quantifying biofilms had used an endpoint, colorimetric assay, such as CV, and that 81% of these had used CV (31).

Electrochemical methods to detect bacteria in real-time have been gaining momentum in the last few years (37–40). One method which has been previously employed to monitor *P. aeruginosa* growth in real-time is square wave voltammetry (SWV) (38). SWV is an electrochemical quantification method which can be carried out using small sensors (0.5 cm), with the measurements solely based on medium dispersion (38). SWV applies a range of potential differences (V) to the system, typically liquid such as growth media, and measures the current output (A). In this way, physiochemical properties of the system in the media can be determined from the analysis of the current output at a potential difference of interest (41,42). For example, the redox active metabolite, pyocyanin, has oxidation peaks at -0.560, -0.311, and 0.699 V (43), also reported at -0.25 V (38), and -0.37 (44). The intensity of the peak positively correlates to the quantity of pyocyanin present in the system (38). Other compounds are also able to be detected by SWV, for example LB growth media has an oxidation peak at 0.85 V (45). Hence, this study was carried out with measurements between -0.5 and 0.5 V. As the potential difference applied is small, it only minimally affects the conditions of the system therefore outputs robust measurements (42). This has allowed SWV to be employed for the detection, identification, and quantification of microorganisms

growing in culture (42). The metabolites the bacteria produce, for example pyocyanin, change the ionic composition of the medium, thereby changing the conductivity of the media, which is measured at the working electrode at a specific potential difference (38,42). Using this, a user can gain information about the charged molecules in the media (38), and monitoring this allows changes to the media to be observed in real-time, *in situ*, and this can be applied to bacteria growing in liquid culture (40,46). As the measurements are based on the dispersion of metabolites within the media, SWV is only able to quantify planktonic growth in real-time, and not biofilm formation.

However, another electrochemical method which has been previously employed to monitor biofilms in real-time is electrochemical impedance spectroscopy (EIS) (11,37–40). EIS has been found to be a rapid and inexpensive point-of-care diagnostic tool, using screen-printed electrodes for less than £2 per sensor (39), and it has even been found to outperform traditional microbiological techniques (39,40). Like SWV, EIS is also non-destructive (11), however instead measures variations close to the electrode surface; the biofilm build up directly on the surface of the sensor (39). For EIS, measurements are based on the electrical impedance on the surface of an electrode. In EIS, a range of frequencies are passed between two electrodes and the impedance modulus (Ω) between the electrodes is measured (47). Using a range of frequencies allows the user to gain information about the resistive and capacitive properties of the system studied, meaning that any build-up of cells or debris on the electrodes from a forming biofilm, is measured as a decrease in impedance modulus (40). Typically, impedance values are fit to a model, such as a Randle's equivalent circuit (37,38,46,48), to extract further analytical parameters (38,39) However changes in raw impedance modulus values have also been employed previously to detect antibiotic resistance between two strains of *S. aureus* (39). Furthermore, these authors employed a normalisation technique for EIS which treats each electrode sensor as a closed system as impedance is sensitive; by normalising each well against its t=0, any variations between sensors are considered. Both SWV and EIS allow for real-time monitoring of bacterial growth (40), therefore EIS has the potential to be of greater benefit for biofilm detection than other methods. (38,39)Raw impedance modulus values have also been demonstrated to be indicative of the biofilm on the sensor (40), providing easier access for point of care, real-time diagnostics.

P. aeruginosa is infamous for its prolific ability to form biofilms in inhospitable environments (6), and its ability to develop antibiotic resistance, as mentioned previously. For example, a review looking at Nepalese clinical isolates found that 42% of *P. aeruginosa* isolates were resistant to two or more antibiotics (49), whilst another study showed more than 55% of *P. aeruginosa* clinical isolates were resistant to 12 antibiotics (50). A large array of genetic adaptations, including horizontal gene transfer (51), and ability to encode a large number of virulence factors (30,51) have contributed to *P. aeruginosa* being the etiological agent of 10% of all recorded nosocomial infections in the European Union (52), as well as being the leading cause of endoscope infections (2), and death amongst cystic fibrosis (CF) patients (53). There are two commonly used laboratory strains of *P. aeruginosa*; PAO1 and PA14 (35). PA14, originally isolated from a burn wound patient (54), has two additional pathogenicity islands to PAO1, and increased virulence (55,56). This work focusses on PA14, as PA14 shows more consistent biofilm formation compared to PAO1 (1). The other *P. aeruginosa* strain used in this work is LESB58, which belongs to the LES group of *P. aeruginosa* isolates, which are the most common strains in cystic fibrosis patients (57). LESB58 was also the first identified *P. aeruginosa* clinical isolate (58), isolated from a CF patient in Liverpool in 1988 (53). LESB58 is a highly virulent strain of *P. aeruginosa*, encoding 99.2% of all known *P. aeruginosa* virulence factors (59). One of the main reasons *P. aeruginosa* was chosen for this study was due to its ability to produce electrochemically active metabolites, such as pyocyanin, which is produced by 90-95% of *P. aeruginosa* isolates (60). Pyocyanin production has been shown to increase with planktonic growth of *P. aeruginosa* within a closed system (38). Furthermore, pyocyanin is reduced at -0.35 V (61), and it is the chemical signal released during the reduction process which is measured (38). It was therefore hypothesized that measuring the bacterially produced pyocyanin could be an accurate method to quantify the planktonic growth of the *P. aeruginosa*. Furthermore, *P. aeruginosa* attachment has been seen within two hours, and plateaued at four hours (22). Therefore, it was hypothesized that biofilm formation of *P. aeruginosa* would be observable within four hours using EIS.

The work presented here aims to design a model system for the monitoring of growth and inhibition of biofilm formation and develop electrochemical methods for biofilm quantification; specifically electrochemical impedance spectroscopy (EIS) and square wave

voltammetry (SWV), alongside 'gold standard' CV as a published point of reference. Specifically, this work was carried out using the clinically relevant pathogen, *P. aeruginosa.* Two strains were chosen due to their laboratory and clinical significance, PA14 and LESB58.

Methods

Bacterial growth and maintenance

Pseudomonas aeruginosa (strains PA14 & LESB58) were cultured from glycerol stocks and streaked onto lysogeny broth (LB) agar and incubated (37 °C, 18 hours, static). Following growth, LB liquid media (5 mL) was inoculated with a single colony and incubated (37 °C, 18 hours, 250 rpm). For bioactivity and biofilm assays, *P. aeruginosa* was diluted to an OD_{600} of 1, unless stated otherwise.

Initial biofilm quantification (cuvettes)

For the initial biofilm quantification, overnight cultures of *P. aeruginosa* (PA14) were diluted to an OD_{600} of 1 and seeded into a 6-well plate (1 mL, carried out in triplicate) (Corning™), and incubated (4 hours, 37 ^{o}C, static). Following this, the biofilm was dislodged by pipetting the media up and down and transferred to a 1 mL cuvette. This was then read on a spectrophotometer at 600 nm. Following this, the protocol was carried out as before, however after the four-hour incubation, the wells were washed with phosphate-buffered saline (PBS) (Sigma). This was achieved by removing the media without dislodging the biofilm, adding 1 mL of PBS to the wells, and removed gently. A further 1 mL was added, and the biofilm was dislodged and read on the spectrophotometer as before.

Biofilm formation and quantification (96-well plates)

Both PA14 and LESB58 were diluted to an OD_{600} of 1 from overnight cultures, added (100 µL) to a clear-walled, clear-bottomed 96-well plate (carried out in triplicate) (Thermo Scientific™) and incubated (37 °C, static) for 4 hours to allow for biofilm formation with minimal media evaporation. Post-incubation, absorbance was measured at 600 nm then the

medium removed, and the wells washed with 100 µL dH_2O. After air-drying (15 minutes, room temperature (RT)), the wells were stained with 0.1% crystal violet (CV) in dH_2O (w/v) for 15 minutes at RT, after which the CV was removed, and two further washes with PBS were carried out, and the plates air dried (15 minutes, RT). To quantify the CV-stained biofilms, 200 µL ethanol (Fisher Scientific, HPLC-grade) (95%, in dH_2O v/v) was added to each well to solubilise the CV and the absorbance read (570 nm). The biofilm formation was normalised using min-max normalisation (62), also called feature scaling, with media only and *P. aeruginosa* only controls to allow the data to be compared to the electrochemical data collected afterwards

Electrochemical biofilm quantification methods

To carry out electrochemical measurements, 96-well plates with three electrode carbon sensors in the base (Metrohm^{TM}) were used for all electrochemical measurements. These were fitted with a circuit board underneath and could be placed directly onto a specialised plate reader (DropSens Connector 96X) to input and measure electrical signals. To achieve this, desired measurements were set up as scripts on PSTrace software (version 5.9) run on a laptop (Lenovo IdeaPad 320S). A potentiostat (PalmSens4 version 1.7) and multiplexer (PalmSens MUX8-R2) were connected in sequence from the laptop to the plate reader, which enabled desired measurements to be carried out in specific wells (selected on the plate reader) in sequence, as each well forms its own circuit. The plate reader was able to operate within the incubator (Panasonic MIR-154-PE). Set up shown in **figure 1**. Biofilms were formed in the 96-well plate with the three-electrode system in the bottom of each well at a seeding density of OD_{600} of 1, as carried out for the CV quantification and described previously. Measurements from each well were taken every 30 minutes for four hours.

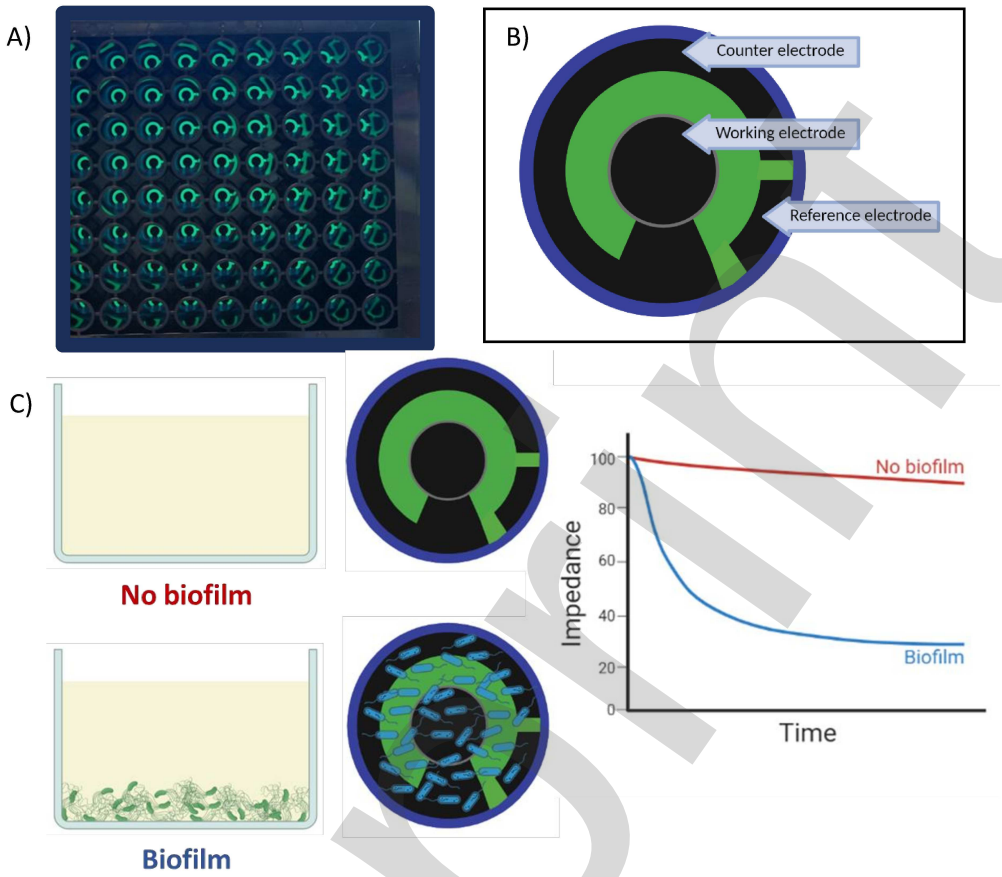
A)
B)
Counter electrode
Working electrode
Reference electrode
C)
No biofilm
Biofilm
Impedance
Time
No biofilm
Biofilm
100
80
60
40
20
0

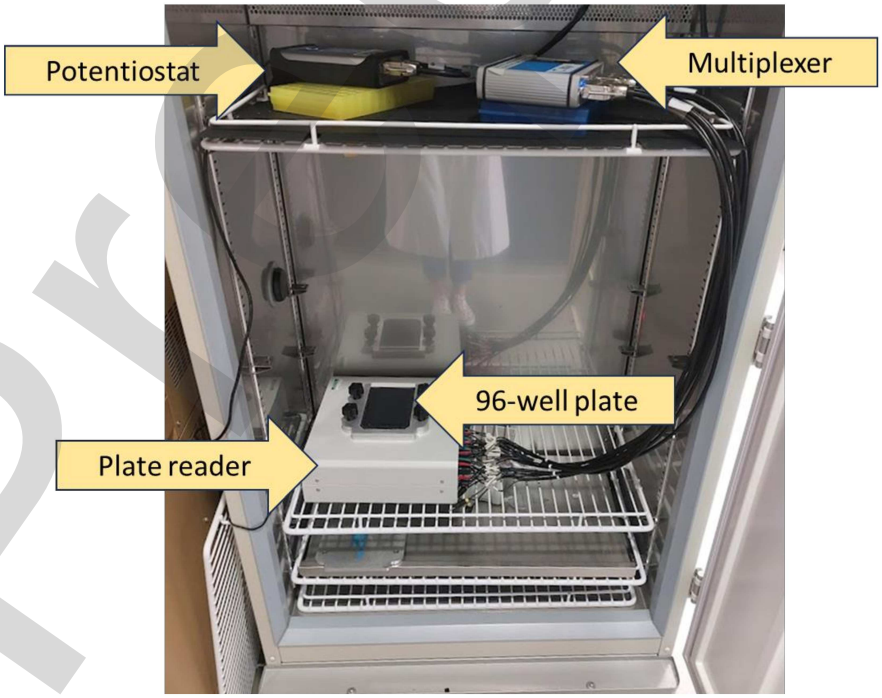
Potentiostat
Multiplexer
96-well plate
Plate reader

208

Figure 1: DropSens™ plate layout and biofilm formation, and equipment set up. A) Close-up of DropSens™ 96-well plate with carbon sensors in the base of each well. **B**) Diagram showing the positioning of the counter, working and reference electrodes on the sensors present in the 96-well plate, C) Schematic of the difference observed when biofilm is present and not present on the sensor, D) Photo taken inside the incubator with a laptop on bench behind the incubator (not seen). The laptop connects directly to the potentiostat, which is connected to the multiplexer on the top shelf. The multiplexer is then connected to the plate reader via 32 inputs. The multiwell plate sits on top of the plate reader; when in use, this is covered with a breathable membrane to maintain sterility. The multiplexer and potentiostat were on blocks to keep them at the same height to reduce strain on the wires.

laptop connects directly to the potentiostat, which is connected to the multiplexer on the top shelf. The multiplexer is then connected to the plate reader via 32 inputs. The multiwell plate sits on top of the plate reader; when in use, this is covered with a breathable membrane to maintain sterility. The multiplexer and potentiostat were on blocks to keep them at the same height to reduce strain on the wires.

Square wave voltammetry (SWV) measurements were carried out with a 5 A current, 3 mV step potential, and 15 Hz frequency. A range of potential differences (-0.5 – 0.5 V) was applied to the wells, and the current output (μA) measured. This gave a peak intensity for metabolites within the media, if they are excited at a potential difference within the range. Peak height positively correlates to the quantity of the metabolite present in the media, thus allowing for quantification. The current at -0.35 V was recorded and used as the planktonic growth measurement. The data was normalised by dividing the respective well by the corresponding t=0 value. In this way, the variations in background noise associated with each sensor were minimised (40).

For electrochemical impedance spectroscopy (EIS) measurements, 0.1 – 10,000 Hz frequencies were scanned at 0.01 V AC potential (11 frequencies per decades at 67 frequencies) and the EIS spectra measured against the open circuit potential. This output of raw impedance modulus (Ω) values was then analysed for trends; both over time at the same frequency, and at a range of frequencies at the same time point. An increase in

biofilm formation on the sensor correlated with a decrease in the impedance modulus at a frequency of 10 Hz. Higher frequencies contained a large amount of noise. The data was again normalised by dividing the respective well by the corresponding t=0 value to minimise the variations in background noise associated with each sensor (40).

Pyocyanin concentration curve

A standard curve was required to identify SWV peak(s) of interest for pyocyanin, therefore pyocyanin (Sigma Aldrich) was dissolved in ethanol (100%) to a concentration of 1 mM. This stock was then diluted in dH_2O to 100 µM, and then serially diluted seven-fold in dH_2O to 0.781 µM. These dilutions were then measured using the same SWV protocol described above; with potential differences between -0.5 and 0.5 V applied to the wells.

Statistical analysis

For all data sets subject to statistical analysis, a Shapiro-Wilk test was performed initially to confirm the dataset was normally distributed. Following the normality test, statistical differences between samples was carried out. For the comparison of two samples, an independent samples t-test was performed. Where there were more than two samples, a one-way ANOVA was carried out to determine if there was significant difference within the group. Following this confirmation, both Tukey's and Dunnet's posthoc tests were carried out, which compared all groups to each other and to the control, respectively. Significance from all tests was determined as ≤ 0.05, except for Shapiro-Wilk, in which ≤ 0.05 indicates that the samples are not normally distributed. All statistical analysis was carried out using SPSS (version 28.0.0.0 (190)).

Results

First, it was important to assess *P. aeruginosa* PA14 growth under the conditions by which biofilm growth would be evaluated (37^{o}C, 4 hours, static). This was done by dislodging the biofilm from the walls of the well (6-well plate), and then measuring the optical density at 600 nm (OD) as a proxy for biofilm growth, as is standard practice for non-filamentous, non-

clumping bacteria. The results showed that OD_{600} ranged from 0.060 - 0.084 with no statistical difference between replicates 1A – 1C ($p \geq 0.05$, n=3) suggesting uniform and consistent measurement (**Table 1**) across all replicates. The final ODs of the biofilm bacteria was unexpected, as the cells were seeded at 0.2 OD_{600}, and therefore an abundance of adhered cells were anticipated. However, to more accurately use this method to quantify biofilm, it would be important to wash the planktonic cells, so that only biofilm cells adhered to the plate surface would be quantified. As such, three PBS washes were introduced and as expected, the cell density was reduced to OD_{600} 0.024, 0.031, and0.081 (**Table 1**), indicating that planktonic cells had been successfully removed. There was also more variation in measurements, with the results being statistically significant from one another ($p \leq 0.05$), including more than a 3-fold difference between replicates 2A and 2C. This suggests that this method is not accurate for biofilm quantification. The main disadvantage of this method, and one that could impact the success in 'capturing' biofilm cells in the measurement, is that pipetting is used to transfer the culture to the cuvette for measurements in the spectrophotometer. There was no method used to determine if all the biofilm cells had been removed from the wells for quantification. This may account for the discrepancies between replicates as well as the low OD_{600} result compared to the seeding density. As such, the results were expected and next the 'gold standard' method of biofilm quantification, CV staining, was assessed. This allowed for biofilms to be quantified within a 96-well plate (necessarily for the chosen electrochemical measurements later) and therefore circumvented the cell-removal issues experienced during OD measurement.

Table 1. Biofilm formation of *P. aeruginosa* quantified spectroscopically. OD_{600} of *P. aeruginosa* (PA14) biofilm after four hours incubation at 37 ^{o}C with (2 A-C) ($p \leq 0.05$, n=3) and without (1 A-C) ($p \geq 0.05$, n=3) PBS washing.

Replicate	OD_{600} (nm)	PBS wash
1A	0.083	No
1B	0.060	No

293	1C	0.084	No
294	2A	0.081	Yes
295	2B	0.031	Yes
	2C	0.024	Yes

Following on from the initial biofilm formations in 6-well plates, decreasing seeding ODs of *P. aeruginosa* (PA14) were introduced to observe if decreasing quantities of biofilm could be detected. The lack of staining in the CV control after the biofilms were washed, confirmed that both the planktonic cells and the background stain were removed, as well, there was a visual decrease in the quantity of stain for decreasing OD_{600} of *P. aeruginosa*.

From this, it was necessary to quantify the CV-stained biofilm, and therefore 95% ethanol (v/v) was used to solubilise the biofilm-bound CV. The biofilms were formed from seeding densities of 0.05 – 1 OD_{600}. The addition of ethanol to the CV-stained wells solubilises the CV from the walls of the wells into the solvent, allowing for spectrophotometric quantification of the CV (**Figure 2**). The CV quantification of both PA14 and LESB58 at increased seeding densities (**Figures 2** and **3**) had clear linear trend lines. As the data was normalised, the end value was 100% biofilm formation, showing an 79.2% increase in biofilm formation between the lowest and highest seeding ODs for PA14. LESB58 showed a 109.7% increase. These both positively correlated to the initial OD that the *P. aeruginosa* were seeded at (r^2 values of 94% and 92%, respectively; indicating the percentage of explained variation of the total variation). Furthermore, there was an overall increase in the standard deviation at the higher starting ODs, particularly compared with those at ODs 0.05 and 0.1 (**Figure 2**). Next, it was of interest to determine if *P. aeruginosa* biofilm formation could be viewed in real-time, rather than as an endpoint, as with CV quantification.

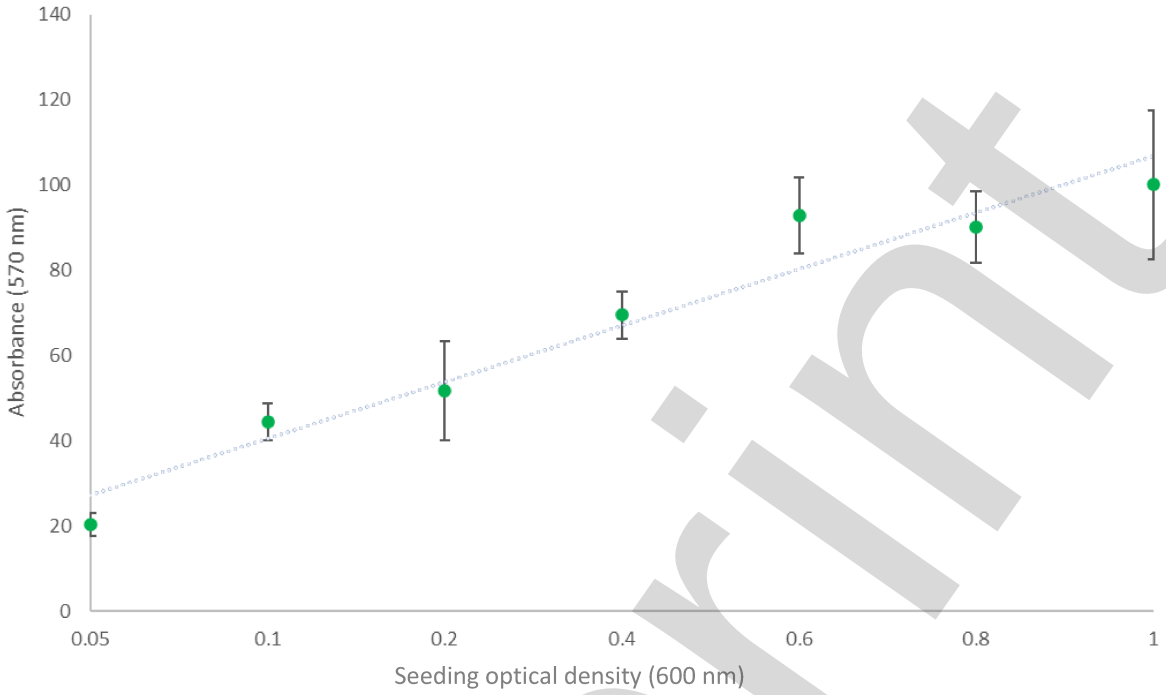

317

318 **Figure 2: Crystal violet quantification of *P. aeruginosa* (PA14) biofilms with increasing**
319 **seeding densities (OD_{600} 0.05 – 1).** Measured after four hours using spectroscopy readings
320 at 570 nm of solubilised CV in ethanol (error bars show standard deviation, n=3, r^2=94%).

321

322

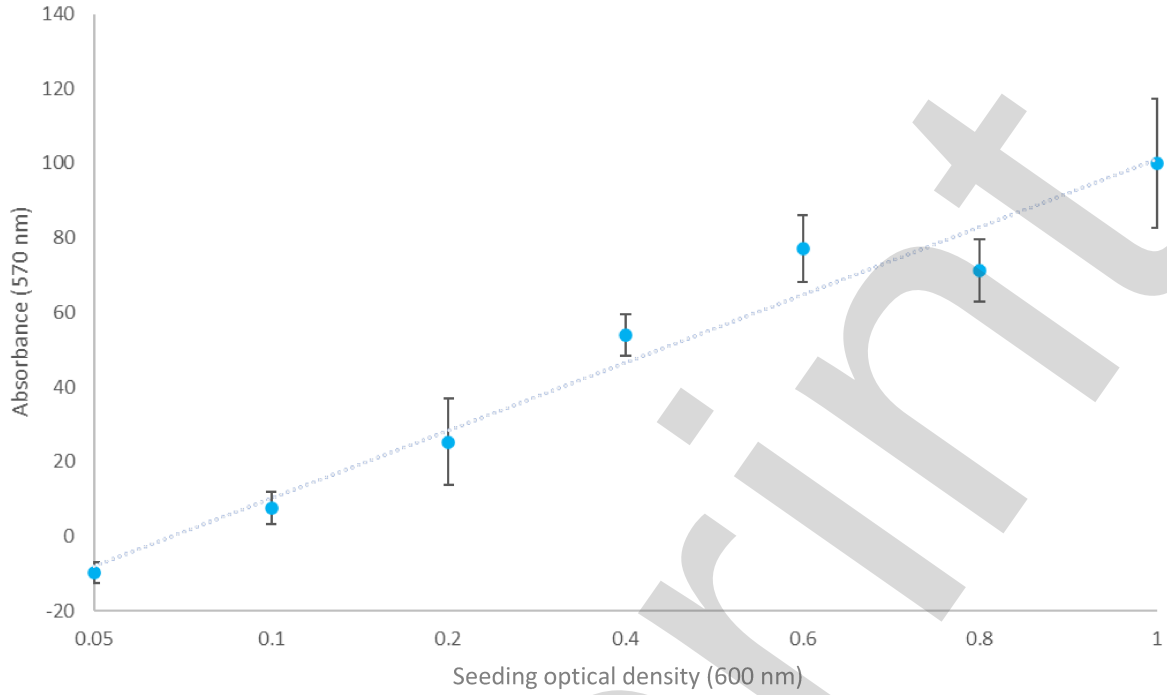

Figure 3: Crystal violet quantification *P. aeruginosa* (LESB58) with increasing seeding densities (OD_{600} 0.05 – 1). Measured after four hours using spectroscopy readings (570 nm) of solubilised CV in ethanol (error bars show standard deviation, n=3, r^2=92%).

As CV quantification provided challenges with accurate and repeatable measurements, as well as only allowing for endpoint reads, we chose to develop methods which enabled electrochemistry to be used to monitor biofilm formation in real-time and *in situ*. As mentioned previously, *P. aeruginosa* produces an electrochemically active secondary metabolite, pyocyanin, which can be measured using electrochemical techniques, used as a proxy for growth (38). Briefly, a range of potential differences (-0.5 – 0.5 V) was applied to the wells, and the current output (µA) measured. Peak height positively correlates to the quantity of the metabolite present in the media, thus allowing for quantification. As proof of concept, increasing concentrations of a pyocyanin standard were quantified using SWV, with a potential difference at -0.35 V, as this is the potential at which pyocyanin is reduced (61), to create a pyocyanin concentration curve (Supplementary **Figure 1**). This has been carried out previously on gold screen-printed electrodes (38), however it was important to carry out this initial concentration curve to show that this also works in this system (carbon screen-printed electrodes). This showed a strong positive correlation between the pyocyanin concentration of a solution and the resulting current (µA) (r^2=99.9%). As pyocyanin production has been shown to increase with planktonic growth of *P. aeruginosa* in a closed system (38), it was therefore hypothesized that measuring the bacterially produced pyocyanin could be an accurate method to quantify the planktonic growth of the *P. aeruginosa*.

As such, the next experiment used the same set-up, but with both *P. aeruginosa* PA14 and LESB58 at increased seeding densities, as carried out earlier. The results showed a similar trend to the CV data (**Figures 4** and 5**,** respectively). As hypothesized from the concentration curve, there was an increased current (μA) output at increased seeding densities (shown as a percentage as the data has been normalised). For example, for PA14, OD 0.05 = 6.4% increase in current, compared to OD 0.8 = 70.6%. Similar trends were seen for LESB58, OD 0.05 = 1.2%, and OD 0.8 = 64.2%. This increased current output demonstrates increased pyocyanin production, and subsequently the density of *P. aeruginosa* cells. As both sets of data were normalised to the current at the highest concentration of pyocyanin (OD_{600} = 1), **Figures 4** and **5** do not show the differences in pyocyanin production between PA14 and LESB58. Looking at the current output data prior to normalisation (**Supplementary Figure 2**), it can be observed that LESB58 produces more pyocyanin than PA14; LESB58 = 12.7 μA, compared to 2.2 μA for PA14, both at OD_{600} 1. This is because LESB58 has increased virulence compared to PA14, and pyocyanin is a virulence factor of *P. aeruginosa*. The pyocyanin concentration curve had an r^2 value of 99.9%, compared to 91% for the SWV data (both PA14 and LESB58); r^2 indicating the percentage of explained variation of the total variation. This is surprising, as the concentration curve in **Supplementary Figure 1** is pyocyanin and media only, whereas *P. aeruginosa* cultures produce other metabolites in addition to pyocyanin. These additional metabolites, such as pyoverdine, add additional variation to these wells, which is not measured by the concentration curve. Next, it was of interest to determine if biofilm formation could be observed over the four hours, rather than an endpoint read, as with CV.

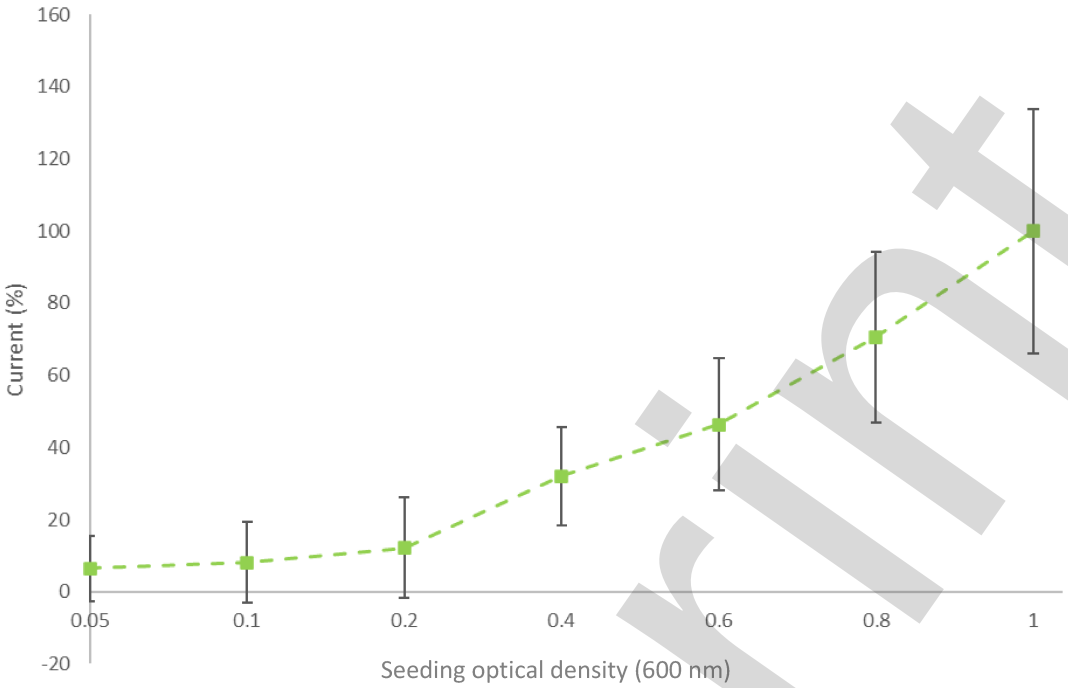

376

377 **Figure 4: SWV quantification of *P. aeruginosa* (PA14) with increasing seeding densities**
378 **(OD_{600} 0.05 – 1).** Current (µA) measured over four hours at -0.35 V, normalised four-hour
379 time point shown (error bars show standard deviation, n=3, r^2=91%).

380

381

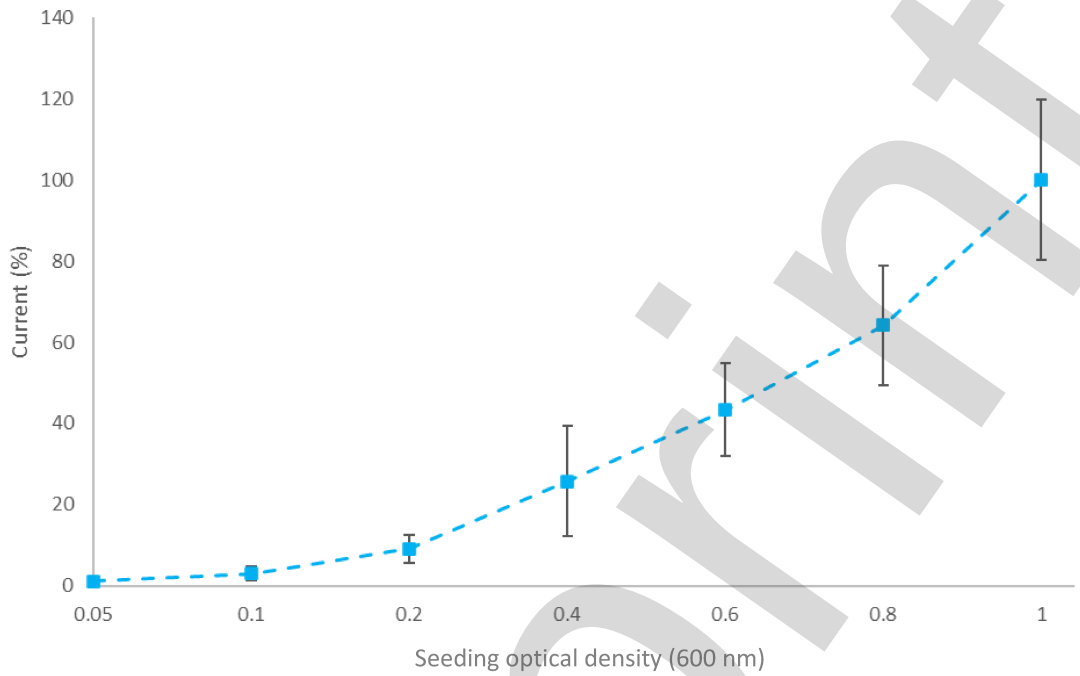

382

383

384 **Figure 5: SWV quantification of *P. aeruginosa* (LESB58) with increasing seeding densities**
385 **(OD_{600} 0.05 – 1).** Current (µA) measured over four hours at -0.35 V, normalised four-hour
386 time point shown (error bars show standard deviation, n=3, r^2=91%).

387

As mentioned previously, SWV measurements at -0.35 V quantify the concentration of pyocyanin within the media (correlating to planktonic growth of *P. aeruginosa*). As such, it was hypothesized that EIS could be employed to quantify biofilm formation, as this instead measured the build-up of cells on the electrode, with a decrease in impedance modulus indicating biofilm formation. As expected, the EIS spectra of PA14 and LESB58 over four hours showed a decrease in normalised impedance modulus (Ω) from 1 to 0.54, and 1 to 0.43 for PA14 and LESB58, respectively (**Figure 6**), indicating that both strains had formed biofilms within the four hours. Furthermore, there was a significant difference observed in the quantity of biofilm formed by LESB58 after 1.5 hour ($p = 0.046$, $n=3$), when compared to 0 hours, and a significant difference in the quantity of biofilm formed by PA14 after just one hour ($p = 0.00033$, $n=3$) (**Figure 6**). Typically, impedance data is fit to a circuit model as a method of normalisation (38,39), however model-fitting was not carried out here, as significant differences between the LB control and both *P. aeruginosa* strains could be observed without this. Instead, the data was normalised, as in a study by Hannah, *et al.* (40), by dividing by the corresponding t=0 value for each condition. Lastly, there was no significant difference in biofilm between either strain of *P. aeruginosa* after 4 hours ($p = 0.076$, $n=3$). This is despite other studies indicating that LESB58 is a superior biofilm former, due to its lack of motility (55), and conversely, **Supplementary Figure 2** which showed that PA14 formed more biofilm when quantified with CV The ability to detect biofilm formation in real-time, and within 90 minutes, for both strains has strong implications in the field of high throughput diagnostics, for example in real-time monitoring of medical implants.

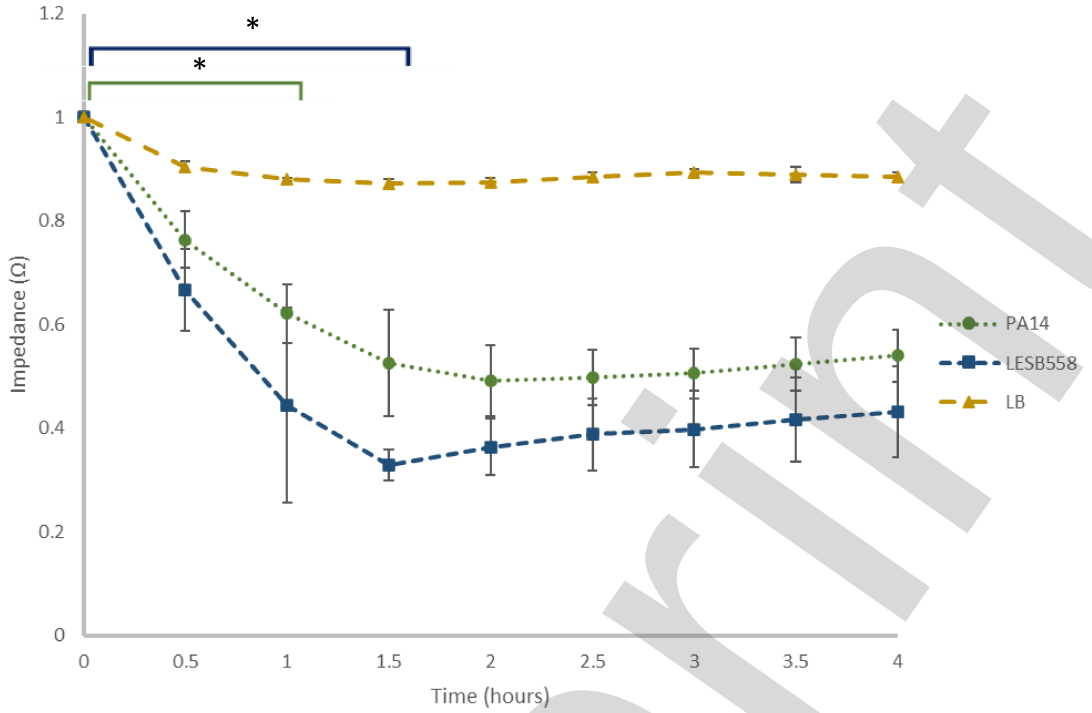

409

410 **Figure 6: EIS quantification of *P. aeruginosa* biofilms over four hours.** PA14 (dark green),
411 LESB58 (dark blue) biofilms and LB media control (dark yellow) quantified using EIS (10 Hz)
412 over four hours. Impedance normalised by dividing each data set by their t=0 value. Error
413 bars show standard deviation, n=3, * denotes significant difference ($p < 0.05$).

414

415 Discussion

416 It has been previously shown that LESB58 forms more biofilm than PA14; a 2005 study compared the
417 biofilm forming ability of environmental isolates to PAO1, another lab strain, and found that 83% of
418 the isolates had up to 18-fold greater biofilm-forming ability than the laboratory strain, with the
419 other 17% having the same biofilm forming ability (9). As well, another study found that LESB58 was
420 able to form 43% more biofilm than both PA14 and PAO1 *in vivo*. Interesting, the site of LESB58
421 infection was in the bronchial lumen; where the infection was initiated (55). The reasoning behind
422 this is potentially due to the reduced swimming and twitching motility exhibited by LESB58 when
423 compared to both PA14 and PAO1 (55). The lack of motility could be attributed to the increased
424 virulence of LESB58, increased virulence is metabolically expensive (59), as seen here with the

increase in pyocyanin production, a virulence factor. In contrast to this, another large study compared more than 200 *P. aeruginosa* isolates taken from humans, as well as animals which have had prolonged, close contact with humans, including dogs and snakes. These *P. aeruginosa* isolates were collected from various human and animal swabs (ear, eye, wound, vaginal, mouth, nasal, and skin) and body fluids (milk, urine, and sputum), and were compared with PAO1 for biofilm formation and human cell pathogenicity. Conversely to the previous studies outlined, only 15% of the *P. aeruginosa* isolates could form biofilms stronger than PAO1, and 5% did not form any biofilm (30). However, the authors do not note where the isolate was taken from; an isolate from a urine sample would possibly be more likely to form biofilm than an isolate from an eye swab due to the environmental pressures the strain finds itself in. For example, LESB58 is an isolate from the cystic fibrosis (CF) human lung (53), and therefore has increased pressures to form biofilm. Furthermore, two of these studies focus on environmental isolates (9,30), rather than clinical isolates, and therefore the strains potentially have decreased virulence due to lesser environmental pressures (63). Lastly, these studies comparing the pathogenicity of different strains quantified biofilm formation using CV, an end-point methodology (9,30,55). Therefore, conclusions with regards to speed of biofilm formation cannot be obtained.

As discussed earlier, there is no standardised method in which biofilms are quantified in the literature, and there is no antibiofilm agent currently available on the US market (1,64). One of the main inconsistencies within the biofilm-quantification community is variations which occur within the CV-staining protocol, despite CV being the most used biofilm quantification method (31). For example, additional PBS washes of the biofilm pre-staining (65), post-staining (56), solvent variation (2), and increased concentrations of CV (21,66). In the one of the earlier studies using CV, in 1998, CV was added directly to the media after the biofilms were grown, resulting in planktonic cells also being stained alongside the biofilm (34). Furthermore, the authors used 1% CV (34), a concentration used in several studies (24,33,34). This is in comparison to the 0.1% used in other studies (1,7,25,35), including this one. Two of the studies which used 0.1% CV, looked at reduction in biofilm formation using amino acids (35), and biofilm growth in different media (1), respectively. Both also included photographs alongside quantification of the biofilms with crystal violet to highlight the background staining. These studies also showed clear trends from the CV data, with similar margins of error as here; and larger error at higher absorbance (570 nm) values. This supports the data, and CV quantification protocol presented here, with a lower concentration of CV as a useful method of biofilm quantification which can inform further

458 assay development with EIS. Lastly, and important for the work carried out here, was that
459 the quantification of biofilm-bound CV is an indirect measurement; the biofilm-bound CV is
460 resolubilised into a solvent and then this is measured (7,66). Here, the aim was to develop a
461 method which could be used to quantify the biofilm as it was forming, rather than an
462 endpoint method, such as CV. This builds upon work previously presented by Dunphy, *et al*.,
463 in which pyocyanin detection was used as a proxy for biofilm formation (38). Here, biofilm
464 formation was able to be measured directly on the sensor, increasing the translatability of
465 the work into other non-pyocyanin producing, biofilm-forming pathogens.

466 Electrochemical measurements, including EIS, have been used to quantify planktonic and
467 biofilm cells previously. As mentioned above, electrochemical data and in particular
468 impedance data, is fit to an equivalent circuit model, such as Randles (38,39,67). However,
469 circuit fitting was not carried out here due to the trends in the data being apparent prior to
470 model fitting. Hannah, *et al*., found similarly, that when measuring the planktonic growth of
471 *E. coli* on their gel-electrode system, there was no requirement for model fitting, and that
472 changes in bacterial growth could be detected from raw impedance modulus values at 100
473 kHz (40). This is highly encouraging, as removal of part of the workflow allows
474 electrochemical methods to be more accessible and therefore increase the likelihood of
475 them being used in the clinical setting by non-specialists. However, the error associated
476 with increased current values could pose issues of reliability in the clinical setting (68).
477 Furthermore, increased variation between measurements and controls has previously been
478 attributed to metabolites within the growth media which are not present in the standards,
479 and increased concentrations of bacteria would hence lead to further variation compared to
480 the standards (38). Another consideration within a clinical setting is the interference of the
481 EIS measurement by sputum, blood, urine, and other body fluids. Recently EIS has been
482 used to detect a cyclic peptide in environmental water samples (69), medicine within
483 patient blood (70), and human protein within simulated urine (71). However, if another
484 sample constituent (other bacteria, macromolecules, drugs) is detected at the same
485 potential during SWV or initiates biofouling, then this would give a false positive. Due to the
486 developed method using two electrochemical methods, this makes the measurements more
487 robust against interferences.

This work has demonstrated the benefit of electrochemical methods over conventional methods, such as CV, but also lesser-used methods, such as hyperspectral imaging. A clear limitation of the study presented here, is the inability to directly measure planktonic growth, instead inferring from the pyocyanin concentration (38). However, previous studies have looked at planktonic only (40), or planktonic in one system and biofilm in another (38), rendering the results incomparable. Therefore, this middle-ground of using both SWV and EIS must be seen as a compromise that will be overcome. Using EIS to monitor *P. aeruginosa* biofilms has previously shown a decreasing impedance as well, with the authors also monitoring capacitance, which is inversely proportional to impedance (72). Furthermore, Kretzschmar, *et al.*, discussed the possibility that carbon electrodes limit the determination of some biofilm properties, due to the increased capacitance associated with the material, and subsequently automatically lowering the impedance measurements (72) when compared to other published data on different electrode materials, such as gold, where impedance data could be read at higher frequencies (25). Lastly, an increased electrical 'noise' has been associated with a multiplexer, which also results in higher EIS frequencies being unusable (47), and therefore studies using single electrodes have been able to monitor higher frequencies (25). These factors may go some way to explaining why the trends in the EIS spectra here were only seen at lower frequencies (10 Hz).

Conclusions

From this work, a standardised method for reliable biofilm quantification of two *P. aeruginosa* strains (PA14 and LESB58) has been achieved using SWV and EIS measurements, further showing that the raw impedance modulus reads could give quantifiable measurements during biofilm formation, rather than endpoint measurements only. This is the first time this has been shown for *Pseudomonas aeruginosa* biofilms without the need for post-measurement model fitting. This advancement makes *P. aeruginosa* biofilm detection more readily accessible and is a huge step towards *in vivo* quantification. *P. aeruginosa* biofilms have been quantified previously using EIS, however as mentioned, importantly the data required circuit fitting (38,73–75). This increases processing time and makes the technology less accessible for non-specialists (38), thereby limiting its use, something this work circumvents. In fact, to our knowledge, the only other instance of

bacterial quantification using the raw impedance values was focussed on *Escherichia coli* (40). The 2020 study demonstrated the use of impedance measurements for phenotypic antibiotic (streptomycin) susceptibility testing (40), and as such, demonstrates another exciting potential for real-world applications. For example, real-time antibiotic susceptibility measurements for isolated strains in clinical settings. In future work, it would be of interest to observe how *P. aeruginosa* responds to antibiotic or antibiofilm agents, and if this can be detected with the developed electrochemical system. Biological replicates of this work would help to improve the accuracy. Lastly, these electrochemical techniques have interesting patient-care applications, and it would be highly worthwhile to assay this with medically relevant materials, as a stepping-stone to point-of-care electrochemical sensing could be used to detect biofilms forming on implanted materials.

Funding

LR and PL were funded through a University of Strathclyde Interdisciplinary Centre for Doctoral Training award in Antimicrobial Resistance (AMR) to KRD, DC, C McCormick and P. Murray.

Acknowledgements

This manuscript reproduces material from a PhD thesis titled 'Identification and quantification of antibiofilm metabolite extracts using electrochemical techniques' (LR, University of Strathclyde).

Conflict of Interest

The authors declare no conflict of interest.

Author Contributions

Funding acquisition KRD, DC; conceptualisation: KRD, DC, LR; investigation: LR, KRD, PL; data curation LR, PL; formal analysis LR, methodology: KRD, DC, LR, PL; project administration KRD; supervision: KRD, DC, writing - original draft LR, KRD; writing – review and editing: LR, PL, DC., KRD.

Data Summary

All data associated with this work is reported within the article.

References

1. Haney EF, Trimble MJ, Cheng JT, Vallé Q, Hancock REW. Critical assessment of methods to quantify biofilm growth and evaluate antibiofilm activity of host defence peptides. Biomolecules. 2018;8(2):1–22.
2. Akinbobola AB, Sherry L, Mckay WG, Ramage G, Williams C. Tolerance of Pseudomonas aeruginosa in in-vitro biofilms to high-level peracetic acid disinfection. Journal of Hospital Infection. 2017;97(2):162–8.
3. Anwar H, Costerton JW. Enhanced activity of combination of tobramycin and piperacillin for eradication of sessile biofilm cells of Pseudomonas aeruginosa. Antimicrob Agents Chemother. 1990;34(9):1666–71.
4. Moskowitz SM, Foster JM, Emerson J, Burns JL. Clinically Feasible Biofilm Susceptibility Assay for Isolates of Pseudomonas aeruginosa from Patients with Cystic Fibrosis. J Clin Microbiol. 2004;42(5):1915–22.
5. Podos SD, Thanassi JA, Leggio M, Pucci MJ. Bactericidal activity of ACH-702 against nondividing and biofilm staphylococci. Antimicrob Agents Chemother. 2012;56(7):3812–8.
6. Wilson C, Lukowicz R, Merchant S, Valquier-Flynn H, Caballero J, Sandoval J, et al. Quantitative and Qualitative Assessment Methods for Biofilm Growth: A Mini-review. Nature Rev Drug Discovery. 2016;5(6):1–8.
7. Kamer AMA, Abdelaziz AA, Al-Monofy KB, Al-Madboly LA. Antibacterial, antibiofilm, and anti-quorum sensing activities of pyocyanin against methicillin-resistant Staphylococcus aureus: in vitro and in vivo study. BMC Microbiol. 2023;23(1):1–19.
8. Donlan RM. Biofilm Formation: A Clinically Relevant Microbiological Process. Clinical Infectious Diseases. 2001;33(8):1387–92.
9. Wang EW, Jung JY, Pashia ME, Nason R, Scholnick S, Chole RA. Otopathogenic Pseudomonas aeruginosa strain as competent biofilm formers. Archives of otolaryngology - head and neck surgery. 2005;131(11):983–9.
10. Fisher RA, Gollan B, Helaine S. Persistent bacterial infections and persister cells. Nature Publishing Group. 2017;15:453–64.

11. Xu Y, Dhaouadi Y, Stoodley P, Ren D. Sensing the unreachable: challenges and opportunities in biofilm detection. Curr Opin Biotechnol. 2020;64:79–84.

12. Kalia VC, Prakash J, Koul S, Ray S. Simple and Rapid Method for Detecting Biofilm Forming Bacteria. Indian J Microbiol. 2017;57(1):109–11.

13. Høiby N, Bjarnsholt T, Givskov M, Molin S, Ciofu O. Antibiotic resistance of bacterial biofilms. Int J Antimicrob Agents. 2010;35(4):322–32.

14. Gilbert-Girard S, Reigada I, Savijoki K, Yli-Kauhaluoma J, Fallarero A. Screening of natural compounds identifies ferutinin as an antibacterial and anti-biofilm compound. Vol. 37, Biofouling. 2021. p. 791–807.

15. Marrie TJ, Costerton JW. Scanning and transmission electron microscopy of in situ bacterial colonization of intravenous and intraarterial catheters. J Clin Microbiol. 1984;19(5):687–93.

16. Siracuse JJ, Nandivada P, Giles KA, Hamdan AD, Wyers MC, Chaikof EL, et al. Prosthetic graft infections involving the femoral artery. J Vasc Surg. 2013;57(3):700–5.

17. Tseng YH, Lin CC, Wong MY, Kao CC, Lu MS, Lu CH, et al. Pseudomonas aeruginosa Infections Are Associated with Infection Recurrence in Arteriovenous Grafts Treated with Revision. Medicina (B Aires). 2023;59(1294).

18. NBIC. National Biofilms Innovation Centre Annual Report 2021. 2021;

19. Cabral DJ, Wurster JI, Belenky P. Antibiotic persistence as a metabolic adaptation: Stress, metabolism, the host, and new directions. Pharmaceuticals. 2018;11(1).

20. Conibear TCR, Collins SL, Webb JS. Role of mutation in Pseudomonas aeruginosa biofilm development. PLoS One. 2009;4(7):e6289.

21. Peeters E, Nelis HJ, Coenye T. Comparison of multiple methods for quantification of microbial biofilms grown in microtiter plates. J Microbiol Methods. 2008 Feb 1;72(2):157–65.

22. Fletcher M. The effects of culture concentration and age, time, and temperature on bacterial attachment to polystyrene. Can J Microbiol. 1977;23(1):1–6.

23. Stiefel P, Rosenberg U, Schneider J, Mauerhofer S, Maniura-Weber K, Ren Q. Is biofilm removal properly assessed? Comparison of different quantification methods in a 96-well plate system. Appl Microbiol Biotechnol. 2016;100:4135–45.

24. Djordjevic D, Wiedmann M, Mclandsborough LA. Microtiter Plate Assay for Assessment of Listeria monocytogenes Biofilm Formation. Appl Environ Microbiol. 2002;68(6):2950–8.

25. Van Duuren JBJH, Müsken M, Karge B, Tomasch J, Wittmann C, Häussler S, et al. Use of Single-Frequency Impedance Spectroscopy to Characterize the Growth Dynamics of Biofilm Formation in Pseudomonas aeruginosa. Sci Rep. 2017;7(1):1–11.

26. Hancock V, Klemm P. Global gene expression profiling of asymptomatic bacteriuria Escherichia coli during biofilm growth in human urine. Infect Immun. 2007;75(2):966–76.

27. Nilsson M, Chiang WC, Fazli M, Gjermansen M, Givskov M, Tolker-Nielsen T. Influence of putative exopolysaccharide genes on Pseudomonas putida KT2440 biofilm stability. Environ Microbiol. 2011;13(5):1357–69.

28. Guiton PS, Hung CS, Kline KA, Roth R, Kau AL, Hayes E, et al. Contribution of autolysin and sortase A during Enterococcus faecalis DNA-dependent biofilm development. Infect Immun. 2009;77(9):3626–38.

29. Dinda AP, Asnani A, Anjarwati DU. The Activities of Streptomyces W-5A as Antibacterial and Antibiofilm towards Methicillin-resistant Staphylococcus aureus 2983. Proceedings of the 1st Jenderal Soedirman International Medical Conference in conjunction with the 5th Annual Scientific Meeting (Temilnas) Consortium of Biomedical Science Indonesia. 2021;(JIMC 2020):109–15.

30. Milivojevic D, Šumonja N, Medić S, Pavic A, Moric I, Vasiljevic B, et al. Biofilm-forming ability and infection potential of Pseudomonas aeruginosa strains isolated from animals and humans. Pathog Dis. 2018;76(4):1–14.

31. Summer K, Browne J, Hollanders M, Benkendorff K. Out of control: The need for standardised solvent approaches and data reporting in antibiofilm assays incorporating dimethyl-sulfoxide (DMSO). Biofilm. 2022;4(August).

32. Kemung HM, Tan LT hern, Chan K gan, Ser H leng, Law JW fei, Lee L han, et al. Streptomyces sp. Strain MUSC 125 from Mangrove Soil in Malaysia with Anti-MRSA, Anti-Biofilm and Antioxidant Activities. Molecules. 2020;25(3545):1–20.

33. Woodward MJ, Sojka M, Sprigings KA, Humphrey TJ. The role of SEF14 and SEF17 fimbriae in the adherence of Salmonella enterica serotype Enteritidis to inanimate surfaces. J Med Microbiol. 2000;49(5):481–7.

34. O'Toole GA, Kolter R. Initiation of biofilm formation in Pseudomonas fluorescens WCS365 proceeds via multiple, convergent signalling pathways: A genetic analysis. Vol. 28, Molecular Microbiology. 1998. p. 449–61.

35. Kao WTK, Frye M, Gagnon P, Vogel JP, Chole R. D-amino acids do not inhibit Pseudomonas aeruginosa biofilm formation. Laryngoscope Investig Otolaryngol. 2017;2(1):4–9.

36. Panda P, Chaudhary U, Dube S. Comparison of four different methods for detection of biofilm formation by uropathogens. Indian J Pathol Microbiol. 2016;59(2):177–9.

37. Domingo-Roca R, Lasserre P, Riordan L, Macdonald AR, Dobrea A, Duncan KR, et al. Rapid assessment of antibiotic susceptibility using a fully 3D-printed impedance-based biosensor. Biosens Bioelectron X. 2023;13:100308.

38. Dunphy RD, Lasserre P, Riordan L, Duncan KR, McCormick C, Murray P, et al. Combining hyperspectral imaging and electrochemical sensing for detection of Pseudomonas aeruginosa through pyocyanin production. Sensors & Diagnostics. 2022;1(4):841–50.

39. Hannah S, Addington E, Alcorn D, Shu W, Hoskisson PA, Corrigan DK. Rapid antibiotic susceptibility testing using low-cost, commercially available screen-printed electrodes. Biosens Bioelectron. 2019;145(July).

40. Hannah S, Dobrea A, Lasserre P, Blair EO, Alcorn D, Hoskisson PA, et al. Development of a Rapid, Antimicrobial Susceptibility Test for E. coli Based on Low-Cost, Screen-Printed Electrodes. Biosensors (Basel). 2020;10(11).

41. Macdonald JR. Impedance spectroscopy. Ann Biomed Eng. 1992;20:289–305.

42. Ramírez N, Regueiro A, Arias O, Contreras R. Electrochemical impedance spectroscopy: An effective tool for a fast microbiological diagnosis. Biotecnología Aplicada. 2009;26(2):72–8.

43. Alatraktchi FA, Andersen SB, Johansen HK, Molin S, Svendsen WE. Fast selective detection of pyocyanin using cyclic voltammetry. Sensors (Switzerland). 2016;16(3).

44. Bellin DL, Sakhtah H, Zhang Y, Price-Whelan A, Dietrich LEP, Shepard KL. Electrochemical camera chip for simultaneous imaging of multiple metabolites in biofilms. Nat Commun. 2016 Jan 27;7.

45. Oziat J, Cohu T, Elsen S, Gougis M, Malliaras GG, Mailley P. Electrochemical detection of redox molecules secreted by Pseudomonas aeruginosa – Part 1: Electrochemical signatures of different strains. Bioelectrochemistry [Internet]. 2021;140:107747. Available from: https://doi.org/10.1016/j.bioelechem.2021.107747

46. Kim T, Kang J, Lee JH, Yoon J. Influence of attached bacteria and biofilm on double-layer capacitance during biofilm monitoring by electrochemical impedance spectroscopy | Enhanced Reader. Water Res. 2011;45:4615–22.

47. Barreiro M, Sánchez P, Vera J, Viera M, Morales I, Dell´Osa AH, et al. Multiplexing Error and Noise Reduction in Electrical Impedance Tomography Imaging. Frontiers in Electronics. 2022;3(March):1–11.

48. Pellé J, Longo M, Le Poul N, Hellio C, Rioual S, Lescop B. Electrochemical monitoring of the Pseudomonas aeruginosa growth and the formation of a biofilm in TSB media. Bioelectrochemistry. 2023 Apr 1;150.

49. Dawadi P, Khadka C, Shyaula M, Syangtan G, Joshi TP, Pepper SH, et al. Prevalence of metallo-β-lactamases as a correlate of multidrug resistance among clinical Pseudomonas aeruginosa isolates in Nepal. Science of the Total Environment. 2022;850(August):157975.

50. Ochoa SA, López-Montiel F, Escalona G, Cruz-Córdova A, Dávila LB, López-Martínez B, et al. Características patogénicas de cepas de Pseudomonas aeruginosa resistentes a carbapenémicos, asociadas con la formación de biopelículas. Bol Med Hosp Infant Mex. 2013;70(2):138–50.

51. Stover CK, Pham XQ, Erwin AL, Mizoguchi SD, Warrener P, Hickey MJ, et al. Complete genome sequence of Pseudomonas aeruginosa PAO1, an opportunistic pathogen. Nature. 2000;406(6799):959–64.

52. De Bentzmann S, Plésiat P. The Pseudomonas aeruginosa opportunistic pathogen and human infections. Environ Microbiol. 2011;13(7):1655–65.

53. Moore MP, Lamont IL, Williams D, Paterson S, Kukavica-Ibrulj I, Tucker NP, et al. Transmission, adaptation and geographical spread of the Pseudomonas aeruginosa Liverpool epidemic strain. Microb Genom. 2021;7(3).

54. Lee DG, Urbach JM, Wu G, Liberati NT, Feinbaum RL, Miyata S, et al. Genomic analysis reveals that Pseudomonas aeruginosa virulence is combinatorial. Genome Biol. 2006;7(10).

55. Kukavica-Ibrulj I, Bragonzi A, Paroni M, Winstanley C, Sanschagrin F, O'Toole GA, et al. In vivo growth of Pseudomonas aeruginosa strains PAO1 and PA14 and the hypervirulent strain LESB58 in a rat model of chronic lung infection. J Bacteriol. 2008;190(8):2804–13.

56. Mikkelsen H, McMullan R, Filloux A. The Pseudomonas aeruginosa reference strain PA14 displays increased virulence due to a mutation in ladS. PLoS One. 2011;6(12).

57. Martin K, Baddal B, Mustafa N, Perry C, Underwood A, Constantidou C, et al. Clusters of genetically similar isolates of Pseudomonas aeruginosa from multiple hospitals in the UK. J Med Microbiol. 2013;62(PART7):988–1000.

58. Cheng K, Smyth RL, Govan JRW, Doherty C, Winstanley C, Denning N, et al. Spread of β-lactam-resistant Pseudomonas aeruginosa in a cystic fibrosis clinic. Lancet. 1996;348:639–42.

59. Winstanley C, Langille MGI, Fothergill JL, Kukavica-Ibrulj I, Paradis-Bleau C, Sanschagrin F, et al. Newly introduced genomic prophage islands are critical determinants of in vivo competitiveness in the liverpool epidemic strain of pseudomonas aeruginosa. Genome Res. 2009;19(1):12–23.

60. Passador L, Cook JM, Gambello MJ, Rust L, Iglewski BH. Expression of Pseudomonas aeruginosa virulence genes requires cell-to-cell communication. Science (1979). 1993;260(5111):1127–30.

61. Webster TA, Sismaet HJ, Conte JL, Chan I ping J, Goluch ED. Electrochemical detection of Pseudomonas aeruginosa in human fluid samples via pyocyanin. Biosens Bioelectron. 2014;60:265–70.

62. Meier NR, Sutter TM, Jacobsen M, Ottenhoff THM, Vogt JE, Ritz N. Machine Learning Algorithms Evaluate Immune Response to Novel Mycobacterium tuberculosis Antigens for Diagnosis of Tuberculosis. Front Cell Infect Microbiol. 2021 Jan 8;10.

63. Faruque SM, Kamruzzaman M, Meraj IM, Chowdhury N, Nair GB, Sack RB, et al. Pathogenic potential of environmental Vibrio cholerae strains carrying genetic variants of the toxin-coregulated pilus pathogenicity island. Infect Immun. 2003;71(2):1020–5.

64. Condren AR, Kahl LJ, Boelter G, Kritikos G, Banzhaf M, Dietrich LEP, et al. Biofilm Inhibitor Taurolithocholic Acid Alters Colony Morphology, Specialized Metabolism, and Virulence of Pseudomonas aeruginosa. ACS Infect Dis. 2020;6(4):603–12.

65. Topa SH, Palombo EA, Kingshott P, Blackall LL. Activity of cinnamaldehyde on quorum sensing and biofilm susceptibility to antibiotics in Pseudomonas aeruginosa. Microorganisms. 2020;8(3).

66. Yahya MFZR, Alias Z, Karsani SA. Antibiofilm activity and mode of action of DMSO alone and its combination with afatinib against Gram-negative pathogens. Folia Microbiol (Praha). 2018;63(1):23–30.

67. Russell C, Ward AC, Vezza V, Hoskisson P, Alcorn D, Steenson DP, et al. Development of a needle shaped microelectrode for electrochemical detection of the sepsis biomarker interleukin-6 (IL-6) in real time. Biosens Bioelectron. 2019;126(September 2018):806–14.

68. Cornish-Bowden A. Fundamentals of Enzyme Kinetics. 4th ed. Fundamentals of enzyme kinetics. Weinheim: Wiley-Blackwell; 1982.

69. Mandal AK, Pal T, Kumar S, Mukherji S, Mukherji S. A portable EIS-based biosensor for the detection of microcystin-LR residues in environmental water bodies and simulated body fluids. Analyst. 2024;

70. Ozkan E, Ozcelikay G, Gök Topak ED, Nemutlu E, Ozkan SA, Dizdar Ö, et al. Molecularly imprinted electrochemical sensor for the selective and sensitive determination of octreotide in cancer patient plasma sample. Talanta. 2023 Oct 1;263.

71. Alharthi SD, Kanniyappan H, Prithweeraj S, Bijukumar D, Mathew MT. Proteomic-based electrochemical non-invasive biosensor for early breast cancer diagnosis. Int J Biol Macromol. 2023 Dec 31;253.

72. Kretzschmar J, Harnisch F. Electrochemical impedance spectroscopy on biofilm electrodes – conclusive or euphonious? Curr Opin Electrochem. 2021;29(April):100757.

73. Chabowski K, Junka AF, Szymczyk P, Piasecki T, Sierakowski A, Mączyńska B, et al. The Application of Impedance Microsensors for Real-Time Analysis of Pseudomonas aeruginosa Biofilm Formation. Pol J Microbiol. 2015;64(2):115–20.

74. Ward AC, Connolly P, Tucker NP. Pseudomonas aeruginosacan be detected in a polymicrobial competition model using impedance spectroscopy with a novel biosensor. PLoS One. 2014;9(3).

75. Hannah AJ, Ward AC, Connolly P. Rapidly Detected Common Wound Pathogens via Easy-to-Use Electrochemical Sensors. Journal of Biomedical Engineering and Biosciences. 2021;8.

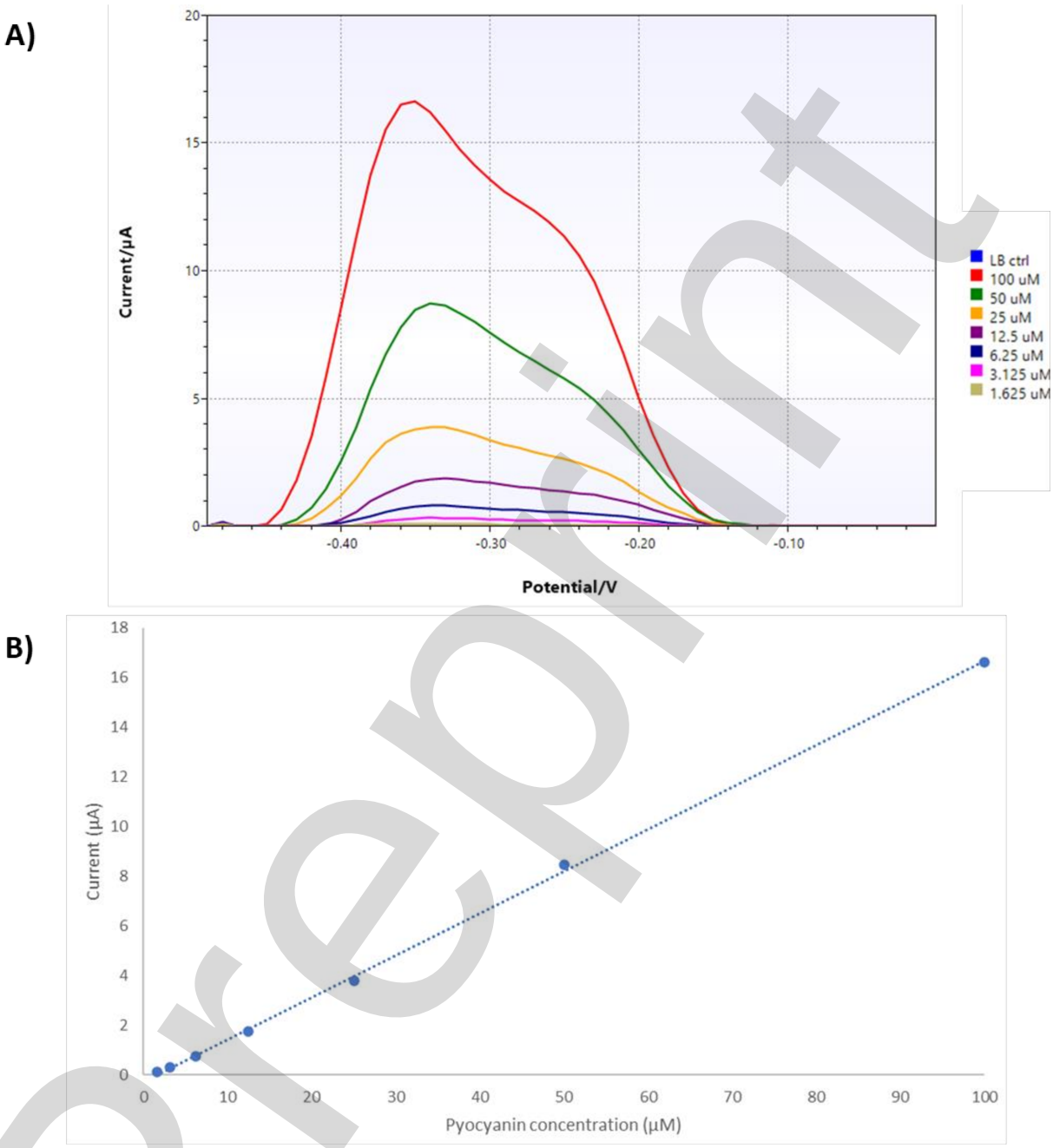

Supplementary Figure 1: SWV Pyocyanin concentration curve. Pyocyanin serial diluted in LB (1.56 – 100 µM) and **A)** measured across a range of potential differences (V). **B)** Corresponding pyocyanin concentration curve showing increasing current output (µA) with increasing pyocyanin concentrations at -0.35 V, r^2=99.9%.

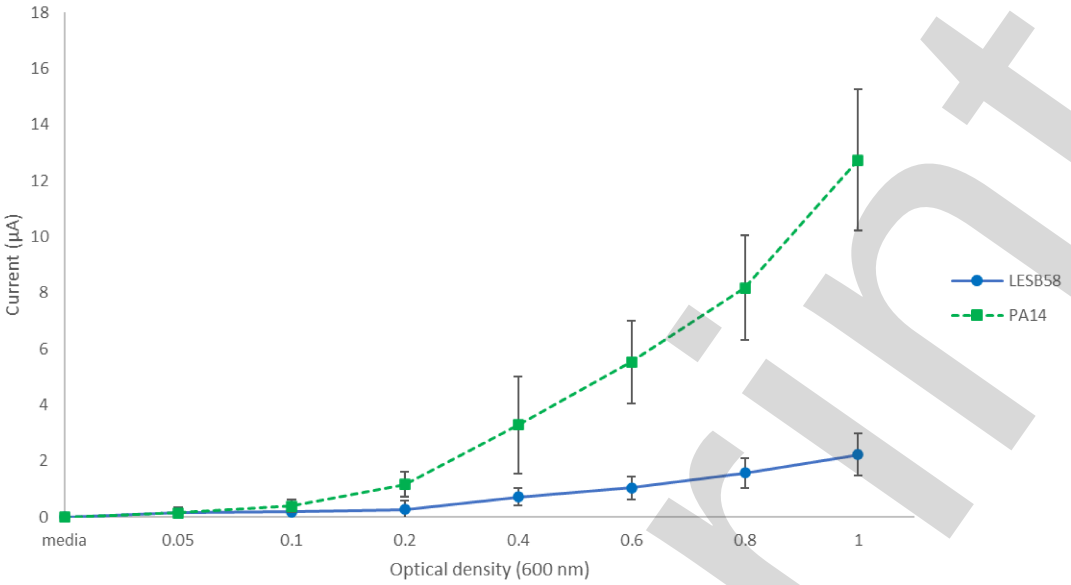

762

763

764 **Supplementary Figure 2: SWV quantification of *P. aeruginosa* (PA14 and LESB58) with**
765 **increasing seeding densities (OD600 0.05 – 1).** Current (µA) measured at -0.35 V over a
766 four-hour incubation, pre-normalised four-hour time points shown (error bars show
767 standard deviation, n=3, r^2=91%).

768

769

770

771

We would like to thank the editor and both reviewers for taking the time to review our manuscript and for the helpful comments and suggestions we have worked hard to address all suggestions, and we believe the paper has been improved as a result of the edits and the work will be useful to the readers of access microbiology.

Editor comments:

During the peer review process, confusion has arisen about the similarity between the results presented in this manuscript and that of some previously published work (Dunphy *et al.* Combining hyperspectral imaging and electrochemical sensing for detection of Pseudomonas aeruginosa through pyocyanin production. Sensors & Diagnostics. 2022;1(4):841–50.). After carefully checking the methods in the two manuscripts, I believe them to be slightly different (HIS vs EIS), but the lack of clarity in this submission on how this method builds upon the previously published method- why is it different? Why is it needed in addition to the other method? etc gives rise to this confusion.

-We thank the editor and the reviewer for this comment and realise we have not been as clear as we should have been about how this work builds on the previously published work - this has now been addressed on lines 19-21 and 469-472.

Additionally, Figure 4 presents an SWV standard curve for pyocyanin as part of method development for using this pigment as a measure of biofilm formation- this method development is already published as part of the Dunphy *et al* paper.

-This was carried out as Dunphy, *et al*. used gold electrodes as opposed to carbon which were used here. This has been explained in lines 342-344, and the figure has been moved to supplemental information.

The conclusions in this submission state that you have developed a standardised method for biofilm quantification using CV staining (line 434-5)- I don't see this in this manuscript. Did the CV staining method require standardisation? Is it not already a well developed and widely used technique with wash steps already included?

-This sentence (line 512) no longer refers to a standardised method for CV biofilm quantification With regard to cv not being standardised – we discuss this on lines 68-71 and reference current literature on this subject highlighting variations, including Haney, *et al.* (2018); Akinbobola, *et al.* (2017); Wilson, *et al.* (2016); Peeters, *et al.* (2008); Kemung, *et al.* (2020); O'Toole & Kolter (1998); Kao, *et al.* (2017); Panda, *et al.* (2016))

The stated benefit to this new method is to show that biofilm can be measured in real time vs endpoint only readings via the CV staining method, but a coherent comparison has not been presented to show the limitation of the CV method for measuring 4-hour biofilm vs this new method.

-Yes, correct – the limitation of CV is that the biofilm can only be measured at a singular time, as stated on lines 332-334, 467-468, and 517-519 – our aim was not to provide a comparison of CV and the methods in this paper at various timepoints as CV is not a standardised method to allow for effective comparison.

The presentation of the data in figures 2-6 is confusing- why set the OD600 = 1 seeding density point as 100% and normalise the other data points to it, rather than present the raw absorbance/current readings for each seeding density? That way the ability of the two methods to detect cells at a lower density would be comparable. Please clarify if the data are from 3 biological or technical replicates. There are many issues with the presentation of the results in this submission. However, I hope that these can be revised to result in a manuscript that contains a useful comparison between this methodology and the standard CV 96-well assay.

-An increased explanation for normalising CV data has been added to lines 186-189, and is explained on lines 232-234 for SWV measurements.

-The direct comparison of the methodologies to quantify lower concentrations of biofilm was outside the scope of the paper – we looked here at the ability to implement a non-destructive method for biofilm quantification. This is stated on lines 17-19, and lines 152-153 have been rephrased to support this.

Reviewer 1:

Major comments:
* A wider range of P. aeruginosa biofilm contexts added to the introduction would strengthen this section and better emphasise the importance of new methods for biofilm quantification (e.g. chronic lung infection, chronic wounds). Similarly, addition of more infection contexts outside of medical devices and implants in the discussion would strengthen the manuscript. Researchers focused on these P. aeruginosa biofilm infections are likely to be interested in the method.

-Further information on *P. aeruginosa* biofilm formation has been added to the introduction, lines 122-139. Information regarding infection context and clinically relevant *P. aeruginosa* models have been added to the discussion, lines 423-447

* A diagram providing an overview of the electrochemical methods described in the introduction would improve the clarity, particularly for those who may be less familiar with these technologies.

-The methodology diagram which served as the graphical abstract has been moved to the methodology section (Figure 1)

* Further discussion of how this method could be used for more clinically relevant P. aeruginosa biofilm models would improve the discussion section, as well as the potential limitations (e.g. would components of artificial sputum media or chronic wound mimicking media be likely to interfere with measurements or is this method a viable option?)

-Clinically-relevant *P. aeruginosa* models were addressed as part of an earlier comment by reviewer 1 – information added to lines 423-447.

-Limitations of measurements with regards to body fluids have been addressed in lines 488-495

Minor comments:
* L229-252. The purpose of this section is slightly unclear as just OD is not a typical method to measure biofilm growth. This section would be improved with a clearer and more concise explanation.

-These lines have been edited to be clearer and more concise. OD_{600} has been used as a typical method to quantify biofilm previously, for example in papers by Bakke, *et al.* (2001) doi:10.1016/s0167-7012(00)00236-0, Joannis, *et al.* (1998) doi:10.1023/A:1008835811731, Larimer, *et al.* (2016) doi:10.1007/s00216-015-9195-z

* Figures 2,3,5 & 6 - improve x axis labels to make it clear this is the seeding optical density.

-These figures have been edited as suggested

Reviewer 2:

The work presented in the manuscript refers to a quantification method of P. aeruginosa biofilms with electrochemical methods. While this paper is presented in another angle, it is very similar to an already published paper (reference 38). This other paper, in which all the authors of the current manuscript are co-authors, presents much more detail to the methods - which I though was somewhat lacking in the current manuscript. Overall, I think this paper lacks adequate depth, and its structure could be improved.

-We have addressed all the comments from the editor and reviewers, and we believe the findings and results are a lot clearer as a result

For instance, the introduction lines 108-118 have some concepts repeated. Also, the authors explore pyocyanin as a proxy for biofilm formation, and electrochemical monitoring without citing other papers with relevant information (for instance https://pubmed.ncbi.nlm.nih.gov/22123963/ and https://pubmed.ncbi.nlm.nih.gov/36509018/).

-These lines have been edited to remove the repetitive line (111-118).

-The reference from Pelle, *et al* (2023), has been added to line 111, as these authors use circuit fitting to measure biofilm formation, as well as presenting imaginary impedance modulus values. The second reference from Koley, *et al* (2011), we do not believe is a necessary addition, as we were not using pyocyanin as a proxy for biofilm growth, instead measuring the biofilm formation directly on the sensor.

Authors also did not use the most common P. aeruginosa laboratory strain (PAO1), not clearly stating the importance of the two strains selected.

-The reasoning behind the strain selection has been added to the introduction, lines 133-139.

The methods are described in a very direct way, however sometimes they are a bit confusing, and it's hard to understand why authors decided to do normalisations when the raw values would work well. A clear example of this is Figures 5 and 6 in which points were normalised but raw data (Figure S1) allows easier comparison.

-This has comment been addressed earlier from the editor

Data in Table 1 was over analysed - particularly the "10-fold reduction" mentioned in lines 239-241. As an example, note that if the treatment changed (PBS wash vs no wash) you can't say that replicates are comparable, and as such they should not be numbered 1-6. There were some oddities in the data as well, like cells seeded at OD600=0.2 then decreasing after 4h incubation (line 236).

-The phrase 10-fold reduction has been removed from line 277

-Table 1 and the corresponding figure heading have been updated so that the difference between replicates is clearer

-The decrease in number of cells has been addressed and expanded upon in lines 285-287

Currently, best practice in plotting data, particularly when no biological replicates are present, just the minimum 3 technical replicates, is that in the plots authors should display all the points to allow better interpretation. Note that increasing technical replicates and including biological replicates could help with what the authors mention in line 294 (challenges with accurate and repeatable measurements).

-Additional replicates have been added to the future work in conclusions, lines 533-534

-We agree that it is informative to plot the three technical replicates, however other papers, for example Paleczny, *et al.* (2023) doi:10.3389/fcimb.2023.1119188, Tello-Díaz, *et al*. (2023) doi 10.1128/spectrum.03931-22, Makhlof, *et* al. (2023) doi:10.1080/09603123.2023.2165045, also plot the average, and we believe is a personal preference, as it has been highlighted to us that the average with the standard deviation is easier to understand

Furthermore, I was somewhat disappointed that after authors presented a good calibration curve for pyocyanin (r2 = 99.9%), they then did not extrapolate an equation to quantify the concentration of pyocyanin from the current measurements, which they say correlates with P. aeruginosa density (line 325). In another part of the discussion, authors note that LESB58 has been shown by other studies to be a superior biofilm former (without references) due to lack of motility. This does not match with the raw data displayed in Figure S1 - one possible explanation is that the experiment was done in a static environment so absence of motility might not have been as relevant, but the authors did not mention this, instead normalising the values and saying they were not different.

-We are not quantifying pyocyanin, we are quantifying biofilm formation – so the extrapolate the equation does not need to be done/

-The lack of motility seen in LESB58 is noted and referenced on lines 409-410

-The comparison between PA14 and LESB58 biofilm formation in figure 7 (now figure 6) normalises the data by removing the strains' respective t=0 value, and hence only removes the background noise. Supplementary Figure 1 (now 2) has been mentioned here (lines 409-411) to improve the explanation.